LIQUID SPRAY COOLING OF A HEATED SURFACE

WILLIAM M. GRISSOM* and F. A. WIERUM

Department of Mechanical Engineering and Materials Science,
Rice University, Houston, TX 77001, U.S.A.

Abstract—The lowest surface temperature possible for the existance of spray evaporative cooling is determined experimentally to be a linear function of the impinging spray mass flux. A conduction-controlled analytical model of droplet evaporation gives fairly good agreement with experimental measurements at atmospheric pressure. At reduced pressures droplet evaporation rates are decreased significantly such that an optimum operating pressure exists for each desired surface heat flux. The initiation of the 'Leidenfrost state' provides the upper surface temperature bound for spray evaporative cooling.

NOMENCLATURE

A_0, initial area of droplet on surface;
$\bar{A}$, time-weighted average droplet area;
A_t, total average area for droplet evaporation;
A_x, area reduction factor;
b, spatially averaged thickness of droplet on surface;
b_0, initial average droplet thickness;
C_p, specific heat of spray fluid;
d, initial diameter of spherical droplet;
d_v, mass-weighted average spherical droplet diameter;
D, 'spread diameter' of droplet on surface;
D_0, initial spread diameter;
$\bar{D}$, time-weighted average spread diameter;
h^*, flooding coefficient;
K, thermal conductivity of spray fluid;
K_m, thermal conductivity of surface material;
$\dot{m}$, spray mass flux impinging on surface;
m, coefficient in relation $b = d^m$;
n, $1 + 2p$ = convenient grouping of terms;
p, $1/2(3/m - 1)$ = coefficient in relation $b = D^p$;
P, surrounding pressure (absolute);
$\bar{P}$, average surrounding pressure for all measurements with a given orifice;
q, surface heat flux;
q^*, surface heat flux required to vaporize all impinging spray mass flux;
q_m^*, maximum surface heat flux possible for the dry-wall state;
t, time measured from beginning of second domain in analytical analysis;
T, temperature within evaporating droplet;
T_0, initial temperature of spray fluid;
T_b, surface temperature at which spray film cooling heat flux exceeds spray evaporative heat flux;
T_f, surface temperature at which flooding state is initiated;
T_s, saturation temperature of spray fluid;
$\bar{T}_s$, saturation temperature corresponding to $\bar{P}$;
T_v, surface temperature at which Leidenfrost state is initiated;
T_w, surface temperature at any time;
x, distance measurement from surface.

Greek symbols

α, thermal diffusivity of spray fluid;
θ, $T - Y_s$;
θ_w, $T_w - T_s$;
λ, latent heat of vaporization of spray fluid;
λ^*, $\lambda + C_p(T_s - T_0)$ = augmented latent heat;
ρ, density of spray fluid;
τ, time measured from droplet impact with surface;
τ_1, time τ at the end of first domain;
τ_2, time t at the end of second domain;
τ_t, $\tau_1 + \tau_2$ = total droplet evaporation time.

INTRODUCTION

THERE are many industrial situations in which a fine liquid spray contacts a surface which is at a temperature in excess of the liquid saturation temperature. The term 'spray cooling' will be used to describe this process. In most such situations the transfer of heat from the surface is the desired effect. In other cases it is a secondary effect; in some situations, it may even be an undesirable side effect.

The purpose of the research reported herein is to identify the fundamental heat transfer processes involved in spray cooling, to provide experimental data useful to the design engineer, and to add to the general understanding of the overall spray cooling process.

The particular application of spray cooling which provided the impetus for this research was the 'Flash Evaporator System' selected by the National Aeronautics and Space Administration (NASA) for use as part of the environmental control system in the Space Shuttle. In this unique application, expendable liquids

* Present Address: Energy Controls Division No. 866, Bendix, 717 N. Bendix Dr., South Bend, Indiana 46620, U.S.A.

are sprayed as a fine mist on the interior walls of a heat exchanger. The walls are heated by the coolant in the environmental control system heat rejection loop. The pressure within the heat exchanger is maintained near the triple point of the spray liquid in order that the lowest possible liquid saturation temperatures may be realized. The latent heat of evaporation required to evaporate the mist at the walls is thus extracted by heat transfer through the walls from the loop coolant. The vapor formed is then rejected to space.

Other applications of spray cooling are encountered in steam generator boiler tubes [1–3] in which water droplets in the two phase flow diffuse to the walls, in the fuel injection and vaporization process in internal combustion engines [4–6], in the cooling of turbine blades [7], in such cryogenic applications as the freeze-drying of foods [8–12], in the spray cooling of hot metals in the steel industries [13], in the spray drying of liquid process streams [14,15], and in liquid metal heat transfer systems encountered mainly in the nuclear power industries [16,17]. Despite this myriad of applications, surprisingly few studies directly concerned with the spray cooling process have been reported.

Three distinct operational modes of spray cooling have been identified. The first is the case in which the surface vaporizes all of the impinging spray. This will be referred to as the 'dry-wall' state and the term 'spray evaporative cooling' will be used to describe the heat transfer process in this mode. Bonacina et al. [18, 19] concentrated on the overall process in this mode, while others [20, 21] have considered the mechanics of the evaporation of a single droplet.

The second operational mode is that in which the spray forms a thin liquid film upon the surface. This will be referred to as the 'flooded' state and the term 'spray film cooling' will be employed to describe the associated heat transfer process. Several studies [22–31] have concentrated on this mode of heat transfer.

The third operational mode is that in which the impinging droplets are deflected from the surface by a thin vapor film which forms on impact. This will be referred to as the 'Leidenfrost' state. There have been numerous studies of the Leidenfrost mode of heat transfer [7, 32–46].

The research reported herein was primarily concerned with the dry-wall state and with the transition from it to the flooded state. The work of Bonacina et al. [18] established the necessary background for the present studies, while elements of the extensive studies of Toda [22] were applicable.

QUALITATIVE ANALYSIS

Of the three operational modes of spray cooling, the dry-wall mode might be considered the most fundamental. The Leidenfrost mode exhibits very poor heat transfer (similar to film boiling), while the flooded mode of operation is essentially that of boiling heat transfer within a thin liquid film, the liquid being

supplied only incidentally by a spray.

The heat flux during the dry-wall operation is directly related to the impinging spray mass flux. Assuming no superheating of the departing vapor

$$q = \dot{m}\lambda^*. \qquad (1)$$

What is of interest is the wall temperature–heat flux range over which the dry-wall mode may exist for a given spray mass flux. Determination of this range is the fundamental problem of spray evaporative cooling and is the primary question addressed in this paper.

Consider the situation in which a spray impinges on a surface at a temperature somewhat in excess of the liquid saturation temperature, with the surface in the dry-wall state, Fig. 1(c). Suppose that, with the spray unchanged, the surface temperature is lowered. At some point, the surface temperature will be too low to evaporate the droplets any faster than they arrive, Fig. 1(b). This is the lower limit for spray evaporative cooling and will be referred to as the 'flooding point'. At a sufficiently lower surface temperature, the full flooded mode of heat transfer would be realized, Fig. 1(a). The surface temperature at which flooding is initiated is quite dependent upon the spray mass flux.

Consider now the possible mechanics of the transition between the dry-wall and flooded states. When the surface just begins to flood at the temperature T_f, Fig. 2(a) small collections of fluid or 'pools' begin to form on the surface. Two distinct situations may result depending upon whether the heat flux through the small pools is greater or less than the heat flux through the surrounding droplets.

Case A—Figs. 2(b), (c) and 3

If the small pools hinder the overall heat transfer through the surface not all of the impinging spray mass can be evaporated with the result that some of the mass accumulates on the surface. Each increase in the pool size would further decrease the surface heat flux, increasing still further the rate of mass accumulation. The result would be a catastrophic change to the flooded state, all at the surface temperature T_f, Fig. 2(c). Mass would continue collecting indefinitely or it would run off the surface in a manner determined by the geometry of the surface. Description of the resulting liquid film thickness and heat transfer process would depend upon surface geometry.

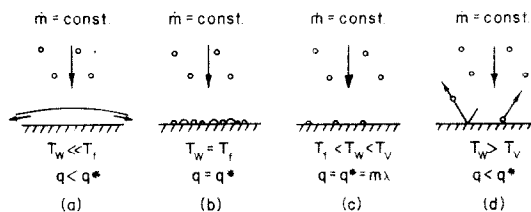To return the surface to its previously dry-wall state,

FIG. 1. The three modes of operation during spray cooling: (a) flooded mode, (c) dry-wall mode, (d) Leidenfrost mode. The transition between (c) and (a) is shown in (b).
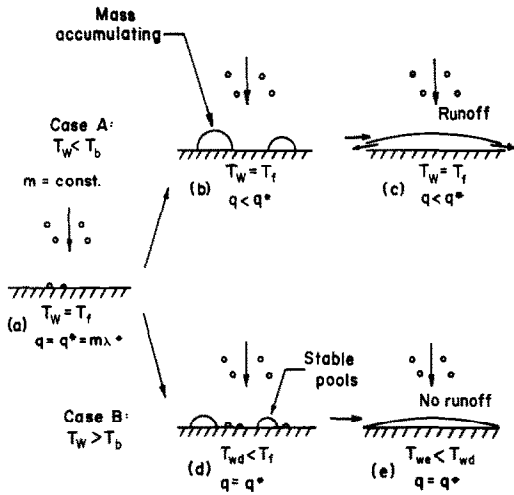
FIG. 2. Mechanism during transition from dry-wall to flooded modes.

the surface temperature must be raised in excess of T_f until such time that the heat transfer through the thin film equals that required by equation (1) to vaporize all of the impinging spray mass flux. This is a hysteresis effect which is not often observed in thermal system.

Case B—Figs. 2(d), (e) and 3

If, on the other hand, the small pools aid the overall heat transfer through the surface, then a stable condition would result. Each decrease in the surface temperature below T_f would increase the pool size. But this increased pool size would, in turn, increase the heat transfer rate, offsetting the decreased surface temperature. At some surface temperature well below T_f the surface would finally be covered completely by a stable thin liquid film. No 'run off' would occur at this point, Fig. 2(e). With further surface temperature decreases, the heat transfer rate would begin to decrease, as described by the spray film cooling curve, and mass would then begin to run off the surface.

FIG. 3. Theoretical predictions. Shaded area gives region for possible spray evaporative cooling operation. For Case A, q_1^* $= \dot{m}_1\lambda^*$, and for Case B, $q_2^* = \dot{m}_2\lambda^*$.

Which of these cases will occur in a given situation is difficult to predict *a priori*. Assume for the moment that the small droplets are evaporated entirely from their surface, with no boiling within the droplets. This would be essentially a conduction-limited phenomenon and, as such, the heat flux would be roughly linear with temperature difference $(T_w - T_s)$. For T_w less than the nucleate boiling temperature the same conduction-limited situation would prevail within the thin liquid pools. However, being much larger than the droplets, the pools should have a much larger thermal resistance. This should guarantee that Case A would result for T_w less than the nucleate boiling temperature.

As T_w is increased past the nucleate boiling temperature, the heat flux through the small pools would increase as a power function of the temperature difference. At some temperature T_b it should exceed the linearly increasing heat flux to the spray droplets. For $T_w > T_b$ then, Case B should result. These cases are outlined in Fig. 3.

Although the effort in this research was not to study spray film cooling in detail, it was necessary to obtain a spray film cooling curve for the surface–liquid pair used in order to determine when each of the above cases would result once surface flooding was initiated.

Consider now the other range limit for spray evaporative cooling, the initiation of the Leidenfrost state. At a sufficiently high surface temperature T_v, an impinging droplet would begin to vaporize at the bottom as it contacted the surface. This would quickly spread into a vapor film which would allow for a partially inelastic collision with the surface, resulting in the droplet rebounding from the surface on impact, Fig. 1(d).

With an overall heat transfer surface area of small extent, most of the droplets which bounce off the surface would not strike it again. All previous research has been with this configuration. For the case of a surface of 'infinite' extent, however, all of the droplets which rebound from the surface must land again at another point on the surface. Analogous to the previous argument, when the surface heat flux falls below that dictated by equation (1), mass will begin collecting on the surface. In this case, the liquid film which formed might very well be in a film boiling state. The formation of a vapor film under an impinging droplet decreases the surface heat flux so dramatically that initiation of the Leidenfrost state on a surface of very large extent would lead quickly to a flooded surface with film boiling.

For spray evaporative cooling considerations, the determination of the surface temperature at which the Leidenfrost state is initiated is of more importance than the heat transfer during the Leidenfrost mode.

Referring to Fig. 3, it is seen that the crux of an experimental analysis rests upon determining the locus of flooding points for spray evaporative cooling. These yield the maximum possible heat flux for each surface temperature during this mode of heat transfer. Also of
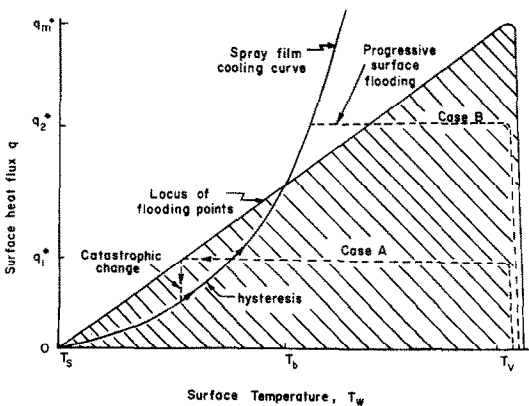
interest, is the determination of the Leidenfrost state temperature T_v, which specifies the uppermost range for spray evaporative cooling, q_m^*. The influence of various other parameters upon these curves is of considerable interest. The effects of surrounding pressure were studied in this research, for water at a constant supply temperature sprayed through a given nozzle onto a polished aluminum surface.

EXPERIMENTAL EQUIPMENT AND PROCEDURE

From the qualitative analysis above it was determined that the two main variables to measure would be the surface temperature and the heat flux through the metal wall upon which the water droplets are impinging. A rather common technique was employed to do this. The axial temperature profile along an aluminum cylinder heated on one end and cooled by a water spray on the other was determined. From this both the heat flux at the surface and the surface temperature could be easily determined. Since the mass flux of droplets onto the surface is proportional to the heat flux (equation 1), it was not necessary to directly measure the flow rate of droplets onto the surface.

The apparatus employed to perform this function is shown schematically in Fig. 4. Heat was supplied by a 300 W commercial cartridge heater. Nine copper-constantan thermocouples were located 6.35 mm apart along the sample centerline in 1.59 mm dia. holes. Wood's metal (m.p. 80°C) was inserted in the holes to ensure excellent thermal contact. An oil-submerged thermocouple in a well-insulated ice bath provided the reference voltage. Voltages were measured with a millivolt potentiometer. The thermocouple nearest (6.35 mm beneath) the surface and the one farthest away were monitored on a chart recorder.
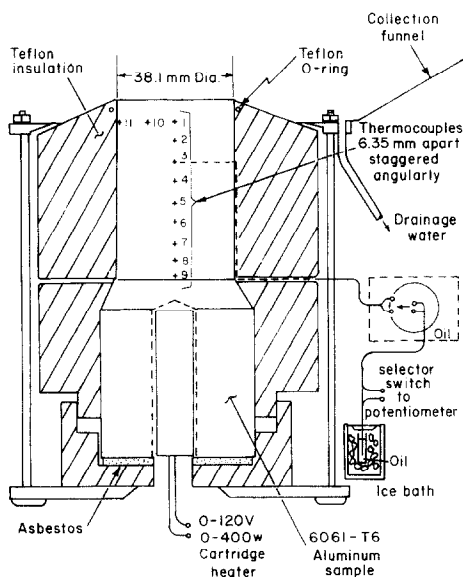
Convective losses at the surface were estimated to be on the order of 0.1–1% of the measured heat flux. Thermal leakage out of the sides and bottom of the aluminum cylinder, while not affecting the measured values of heat flux and surface temperature, did limit the maximum observable surface heat flux. The surface was polished with 00 grade steel wool prior to each run.

For a given spray mass flux it was not possible to manually adjust the electrical power to the heater to exactly match that required to vaporize all of the impinging spray [given by equation (1)]. To realize a steady-state operating condition the electrical power to the heater was adjusted with a temperature-feedback control circuit. The thermocouple nearest the heater (no. 9 in Fig. 4) was used in the control circuit since it allowed the fastest response time.

The following procedure was used to obtain the transition from dry-wall to flooded state. Beginning with the surface in a dry-wall state, the set point to the temperature controller was lowered gradually by small increments until the surface just began to flood. At this time a data point was recorded. This method occasionally resulted in a hysteresis of as much as 2°C due to the on–off nature of the commercial temperature controller. On such occasions, an alternate method was to adjust the heater voltage manually so that the aluminum cylinder would cool very gradually. This generally allowed a rapid, 'simultaneous' reading of the thermocouples at the flooding point.

Distilled water at 25°C was sprayed through a 0.40 mm dia., 90° included angle, full-cone nozzle located approx. 45 cm above the surface. To obtain a fine mist spray required a total flow rate far in excess of that which could be completely vaporized by the aluminum surface. The amount of spray impinging on the surface was adjusted by varying the angular orientation of the nozzle without changing the flow rate through the nozzle. Excess water was collected in a large funnel and drained away. For the nozzle flow rate used, the mass-weighted average droplet diameter (determined by optical measurement of droplets collected on a thin oil film) was 155 μm at atmospheric pressure.

The heat flux apparatus, the spray system, and the excess spray collection apparatus were positioned on the base plate of the vacuum system. The various leads were taken through this base plate.

The vacuum system consisted of a 46 cm dia. 76 cm high glass bell jar with stainless steel base plate. A large liquid nitrogen cold trap froze the vapor generated. An orifice plate placed in the exit duct from the bell jar 'choked' the exiting vapor flow. By using different size orifices the pressure under the bell jar was maintained within different distinct pressure ranges. The saturation temperature under the bell jar was measured by placing a thermometer such that it was continually wetted by the spray. This reading always agreed well with the saturation pressure measured by one of three different pressure measuring instruments. The entire
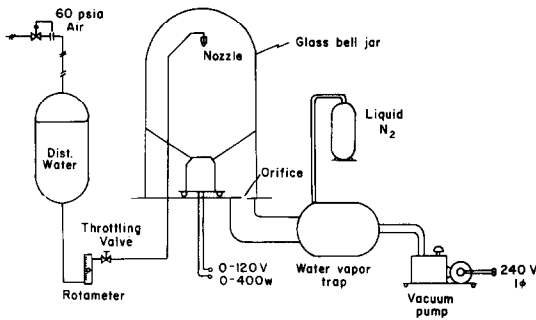

FIG. 4. Schematic diagram of the heat flux sample.

FIG. 5. Schematic diagram of vacuum system and liquid spray supply.

experimental apparatus is depicted schematically in Fig. 5.

Spray film cooling measurements for the 'flooded state' were made by supplying a heat flux to the aluminum cylinder and adjusting the spray so that a flooded condition existed with only a minimum amount of runoff. The surface temperature determined under these conditions was simply that needed to balance the imposed heat flux as in any boiling heat transfer experiment.

EXPERIMENTAL RESULTS

Flooding locus measurements

The measurements of the flooding point at atmospheric pressure are given in Fig. 6. It should be noted that no physical restrictions prohibit a steady-state condition from existing to the right of this flooding locus curve. The determination of the flooding point was a subjective visual determination and limited by the experimenters determination that the surface was just on the verge of flooding rather than being simply an 'accuracy of experimental instruments' type of measurement. Most of the scatter in the data is believed to be due to the inability to maintain a truly steady spray mass flux upon the sample surface. The 'best fit' line shown in Fig. 6 was drawn linear in the

high heat flux region, intersecting the origin. The deviation of the measurements from this linear fit in the low heat flux region is attributed to evaporation to the unsaturated room atmosphere (r.h. 50%). At the higher heat fluxes the atmosphere directly over the sample becomes almost saturated with the large amount of vapor generated.

All of the atmospheric measurements taken during this study as well as the only known measurements by other researchers were compared with the flooding locus from Fig. 6 [48]. Not surprisingly, few of the measurements fell to the left of the flooding locus determined here as should be the case since the flooding locus is simply the lower limit for the existence of the 'dry-wall' mode of operation.

The majority of the low-pressure measurements were carried out using a 9.53 mm dia. orifice in the vacuum line. This provided a pressure range (about 6.76 mm Hg) slightly above the triple point of water (4.59 mm Hg). The results obtained using this orifice are given in Fig. 7. The pressure associated with each orifice is taken as the average pressure of all of the measurements with that orifice. The measurements display a much better correlation than those at atmospheric pressure. This is believed to be due to the much steadier spray mass flux obtained in the absence of appreciable atmospheric disturbances.

Runs were made with two additional orifice plates which provided mean pressures of 4.56 and 19 mm Hg. The correlation of the data for both was very similar to that in Fig. 7.

All of the data taken here may be summarized, as shown in Fig. 8, by defining a 'flooding coefficient'

$$h^* = \frac{q^*}{(T_f - T_s)} \qquad (2)$$

which is simply the slope of each flooding locus. Considering the saturation temperature as the independent variable, rather than the operating pressure, yields a much simpler plot and aids in the interpretation.
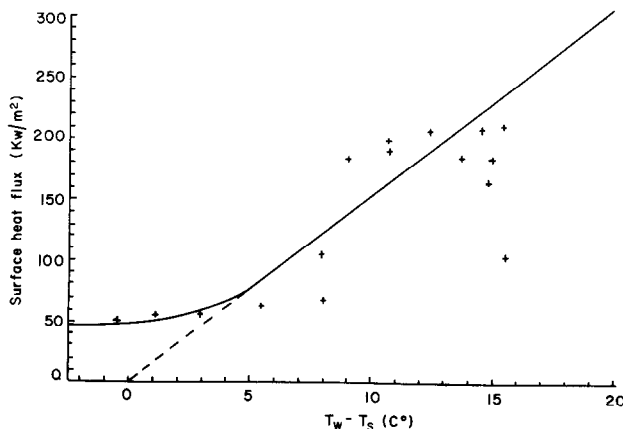

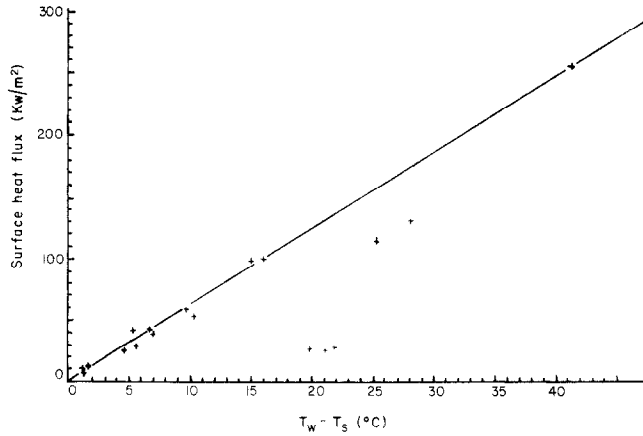FIG. 6. Measurements of the flooding locus at atmospheric pressure.

FIG. 7. Measured flooding locus for $\bar{P}$ = 6.76 mm Hg.

For the designer, the variable of interest would be the actual wall temperature T_w rather than $T_w - T_s$. One important concern to the design engineer would be to determine the operating pressure which would yield the largest attainable heat flux without flooding. Indeed, Fig. 8 suggests that the lowest attainable pressure might not be the most desirable, since the slope of the flooding locus decreases with decreasing operating pressure.

To analyze this, the data of Fig. 8 may be converted back into one similar to Figs. 6 and 7, but with T_w as the abscissa. Several flooding loci constructed by this technique are shown in Fig. 9. If this is continued for infinitesimal increments in saturation temperature, the optimum operating pressure for a given heat flux may be determined. The result is shown in Fig. 10.

Spray film cooling measurements

The spray film cooling measurements taken during operation in the 'flooded' mode at atmospheric pressure gave a well correlated curve which appeared to be independent of the film thickness. Indeed the same results might have been obtained had the liquid film been of infinite thickness (i.e. pool boiling). The

resulting heat-transfer curve is given as a part of Fig. 11.

The spray film cooling mechanism at vacuum pressures appears to be distinctly different from that at atmospheric pressure. The results are omitted here for brevity, but the mechanism appears to be totally conduction-controlled and devoid of any nucleate boiling region [48].

Leidenfrost state temperature

Several rather rough measurements at atmospheric pressure determined

$$T_v - T_s = 38 \pm 14°C, \quad P = 1 \text{ atm.,}$$

while Zodrow [47] determined

$$T_v - T_s = 39 \pm 6°C, \quad P = 1 \text{ atm.}$$

Several more careful measurements at vacuum pressures determined

$$T_v - T_s = 78 \pm 6°C, \quad \bar{P} = 6.76 \text{ mm Hg} \, (\bar{T}_s = 5.75°C).$$

The majority of the references in the literature on the Leidenfrost phenomenon are concerned with the initiation of stable film boiling underneath a rather large
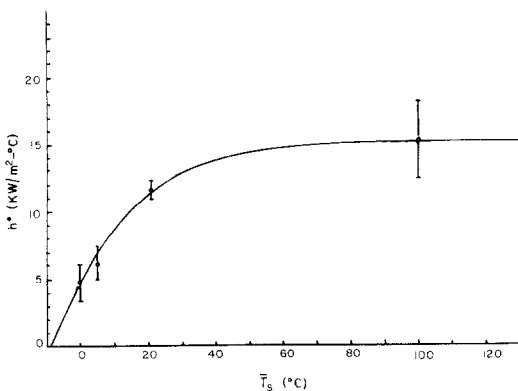

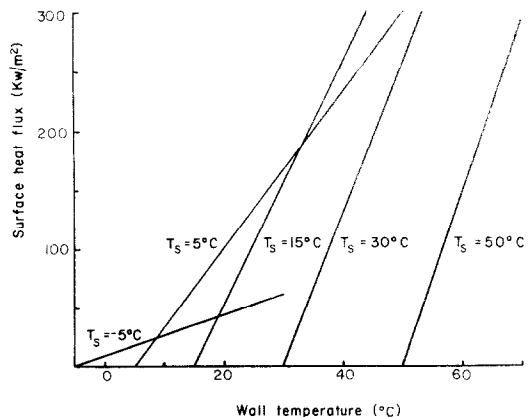FIG. 8. h^* as a function of $\bar{T}_s$.

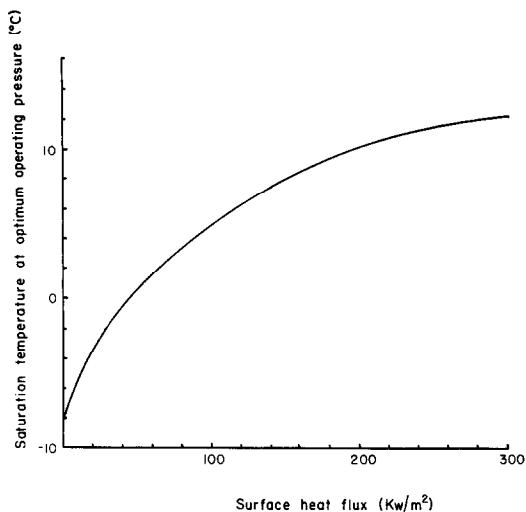
FIG. 9. Data of Fig. 10 reconstructed for design purposes.

FIG. 10. Operation pressure which permits the lowest surface temperature.

sessile drop. This temperature, defined as the 'Leidenfrost Point' is generally about 200°C above saturation of water. It does not seem to predict at all when a small impinging droplet will bounce off of the surface.

Overall range of spray evaporative cooling

If the linear evaporation mechanism is assumed to continue for approximately three times the range considered here, then the overall range for spray evaporative cooling at atmospheric pressure would be as shown in Fig. 11. The maximum possible heat flux is found to be

$$q_m^* = 590 \pm 150 \, \text{KW/m}^2$$

$$(1.87 \pm 0.5 \times 10^5 \, \text{B.t.u./h-ft}^2) \quad \text{at } P = 1 \, \text{atm.}$$

while for vacuum pressure operation

$$q_m^* = 485 \pm 125 \, \text{KW/m}^2 \quad \text{at } \bar{P} = 6.76 \, \text{mm Hg}.$$

It appears, then, in spite of significant changes in h^* and $(T_v - T_s)$ with pressure, the quantity $q_m^* = h^*(T_v - T_s)$ remains essentially the same.

The experimental results in Fig. 11 essentially confirm the major predictions of the qualitative analysis. Hence, there is every indication that the mechanism is as described there. The shaded region gives the range for the existence of the dry-wall mode.

ANALYTICAL ANALYSIS

The linear flooding loci determined experimentally tend to suggest that a conduction-controlled droplet evaporation model might adequately describe the process. This will be considered here.

Saburo Toda [22] presents a very simplified analysis for the evaporation time of a 'liquid film formed from a droplet'. The most significant shortcoming in Toda's analysis is that he uses it to analyze his experimental measurements which were definitely in the 'flooded state'. He describes runoff from the surface and shows the same in photographs.

The excellent agreement of his analytical analysis with his experimental results appears to be a result of having used his experimental data to evaluate four undetermined constants in the analytical analysis. This appears to be a form of having curve-fitted the analytically developed relationship to the measured experimental data.

Toda's most useful experimental result for the present study was his relationship for the average thickness of a droplet resting upon a glass surface. His result was:

$$b = Cd^m, \tag{3}$$

where $m = 0.6$, $C = 2$ for b and d in μm.

Yang [20] develops the equations to be solved to determine the evaporation time for a drop on a solid surface, however he does not solve these equations. His main result is that he determines by an order of magnitude argument that the thermal properties of the
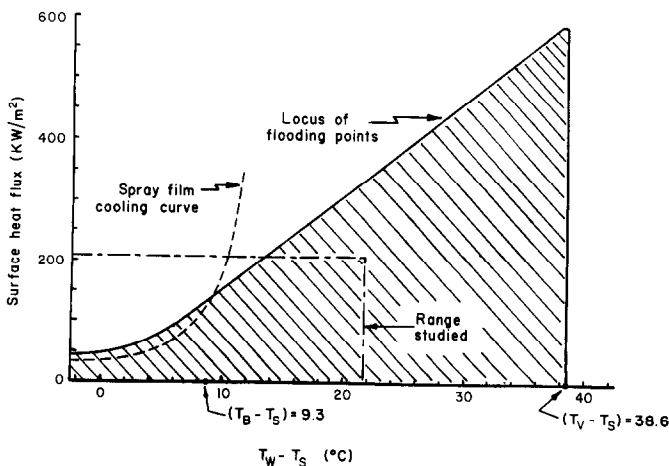

FIG. 11. Overall spray evaporative cooling range at atmospheric pressure assuming continued droplet evaporation without internal boiling. Shaded area gives region for possible spray evaporative cooling operation.
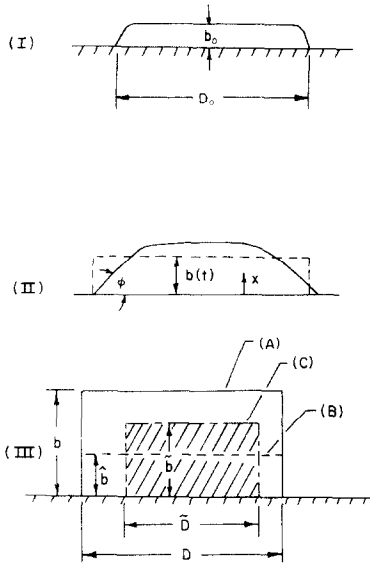
FIG. 12. (I) Initial droplet shape. (II) Droplet during second period of evaporation. (III) Effect of mass removal at droplet surface upon thickness.

surface are not important for $K/K_m \ll 1$. The same result is arrived at in reference [48]. It will be assumed here that this is the case such that the surface temperature under an evaporating droplet remains constant. This might not be the case for a liquid metal spray.

Overall energy balance

Consider first the overall energy balance for an evaporating droplet [Fig. 12 (I)], modeled as a thin right circular cylinder of liquid. At the onset of flooding, as soon as this droplet evaporates another arrives to replace it. The heat transfer at this point is then

$$q^* = \frac{\text{(total energy transferred)}}{\tau_t A_t} \qquad (4)$$

where the total energy transferred $= \rho b_0 A \lambda^*$, $\tau_t =$ total time to evaporate the droplet, and $A_t =$ average surface area occupied by the droplet.

For a square lattice of droplets upon the surface $A_t = 4A_x A_0/\pi$, where $A_x = (\bar{D}/D_0)^2 =$ area reduction due to shrinkage and the $4/\pi$ accounts for the dry region between droplets. Equation (4) then becomes

$$q^* = \frac{\pi \rho \lambda^* b_0}{4 \tau_t A_x}. \qquad (5)$$

Time to evaporate a single droplet

Referring to Fig. 12(I) and (II), the solution must be broken into two domains: The first with an adiabatic upper boundary, and the second with a moving phase front at the upper boundary.

Adiabatic boundary. This domain lasts until the surface temperature of the droplet is raised to the

saturation temperature. Carslaw and Jaeger [49] give the exact solution as:

$$\frac{T - T_0}{T_w - T_0} = \sum_{n=0}^{\infty} (-1)^n \operatorname{erfc}\left[\frac{(2n+1)b_0 - x}{2(\alpha\tau)^{1/2}}\right]$$
$$+ (-1)^n \operatorname{erfc}\left[\frac{(2n+1)b_0 + x}{2(\alpha\tau)^{1/2}}\right]. \qquad (6)$$

The duration τ_1 of the first domain is obtained by solving (6) for $\tau = \tau_1$ with $x = b_0$, $T = T_s$.

Moving phase front boundary. An approximate integral solution will be employed here [50]. Define $t = \tau - \tau_1$. The governing equation is

$$\frac{d}{dt} \int_0^{b(t)} \theta(x,t)dx + \alpha \frac{\partial\theta}{\partial x}\bigg|_{x=0} - \alpha \frac{\partial\theta}{\partial x}\bigg|_{x=b(t)} = 0 \qquad (7)$$

where $\theta = (T - T_s)$, and $\alpha = K/\rho c_p$.

In the appendix it is shown that an energy balance at the surface will yield

$$\rho\lambda n \frac{db}{dt} = K \frac{\partial\theta}{\partial x}\bigg|_{x=b(t)} \qquad (A.5)$$

where n is related to the m in equation (3) by $n = 3/m$.

Assuming a parabolic temperature profile with the boundary conditions $\theta(0,t) = \theta_w$ and $\theta(b,t) = 0$, equation (7) becomes

$$-b'' = \frac{2}{b}(b')^2 + \left(12\alpha - \frac{2K\theta_w}{\rho n\lambda}\right)\frac{b'}{b^2} + \frac{12\alpha K\theta_w}{\rho n\lambda b^3} \qquad (8)$$

where $\theta_w = (T_w - T_s)$, $b' = db/dt$, and $b'' = d^2b/dt^2$, with the initial conditions $b(0) = b_0$ and $b'(0) = 0$.

An approximate closed form solution of (8) is obtained when the higher order terms b'' and $(b')^2$ can be neglected. The resulting approximate solution is

$$b^2(t) = b_0^2 - 12\alpha t \left(\frac{6n\lambda}{c_p\theta_w} - 1\right)^{-1}. \qquad (9)$$

From this the duration τ_2 of the second domain is obtained by setting $b(\tau_2) = 0$

$$\tau_2 = \frac{b_0^2}{12\alpha}\left(\frac{6n\lambda}{c_p\theta_w} - 1\right). \qquad (10)$$

For the present case $\tau_2 \gg \tau_1$ (2% maximum error) and $6n\lambda/c_p\theta_w \gg 1$ (0.2% maximum error). Hence the time to evaporate a single droplet becomes

$$\tau_t = \tau_1 + \tau_2 \simeq b_0^2 n\lambda/2\alpha c_p\theta_w. \qquad (11)$$

$\bar{D}$ is defined as

$$\bar{D}^2 = \frac{1}{\tau_t}\int_0^{\tau_t} D^2(t)dt. \qquad (12)$$

In the appendix it is shown that $D(t) \sim b^p(t)$, where $p = (n-1)/2$, so that

$$\frac{D(t)}{D_0(t)} = \left[\frac{b(t)}{b_0(t)}\right]^p.$$

Substitution in (12) and completing the integration then gives

$$A_x = 1/(p + 1). \tag{13}$$

Total solution

Substituting these relations for τ_t and A_x into (5) and using the definition (2) for h^* gives

$$h^* = \frac{\pi K \lambda^*}{2 b_0 \lambda} \left(\frac{p + 1}{2p + 1} \right). \tag{14}$$

At atmospheric pressure the measured average droplet diameter of 155 μm would give $b_0 = 41$ μm from (3). With $m = 0.6$, equation (A.3) gives $p = 2$. Substitution of these values into (14) along with the appropriate property values of water at 100°C yield $h^* = 18.0$ kW/m^2 $-$ °C. This is 17% larger than the experimentally determined value of 15.4 $\pm$ 3 kW/m^2 $-$ °C at atmospheric pressure.

A numerical solution of equation 8 was performed using the Milne variable step integration technique with IBM's Continuous Systems Modeling Program. The results for saturated water were $h^* = 15.73$ kW/m^2. For this condition equation (14) would predict $h^* = 15.63$ kW/m^2. Hence the approximate closed form solution appears to provide sufficient accuracy for the conditions studied here.

It was not possible to compare the analytical expression with the low pressure data as no relationship such as equation (3) is available for these conditions and the average droplet diameter for the low pressure runs was not determined.

CONCLUSIONS

Over the range of heat fluxes considered here the spray evaporative cooling mechanism appears to be that of conduction-controlled heat transfer through the droplet with evaporation only at the droplet surface. The question of whether boiling within a droplet is initiated before the Leidenfrost state temperature is reached is a very important one which is left unanswered here due to the limited range considered.

The effect of decreasing the surrounding pressure is quite marked. Apparently as a result of decreased 'wettability' of the liquid on the aluminum surface the flooding coefficient, h^*, decreases while the Leidenfrost state temperature $T_v - T_s$ increases, resulting in $q_m^* = h^*(T_v - T_s)$ remaining essentially constant.

Spray film cooling at atmospheric pressure appears to behave the same as ordinary pool boiling. However, at vacuum pressures the mechanism appears to be one of conduction through the liquid film with no nucleate boiling within the film.

REFERENCES

1. L. L. Levitan and F. P. Lantsman, Investigating burnout with flow of a steam–water mixture in a round tube, *Thermal Engng* **22**, 102 (1975).
2. J. P. Parker and R. J. Grosh, Heat transfer to a mist flow, U.S.A. E.C. Report No. ANL-6291 (1961).
3. M. M. Fikry, Heat transfer to wet steam flowing in a horizontal tube, Ph.D. Thesis, Univ. of London (Oct. 1952).
4. H. Hiroyasu, T. Kadota and T. Senda, Evaporation of a fuel droplet contacting with a hot surface in a pressurized and heated ambient gas, *Trans. Japan Soc. Mech. Engrs* **39**(328), 3779 (1973).
5. Z. Tamura and Y. Tanasawa, Evaporation and combustion of a drop contacting with a hot surface, in *7th Symposium (International) on Combustion*, p. 509. Butterworth's, London (1959).
6. W.-J. Yang, Vaporization and combustion of binary liquid drops on heated surface, in *Proc. 1977 Tokyo Joint Gas Turbine Congress*, p. 77 (1977).
7. P. Savic and G. T. Boult, The fluid flow associated with the impact of liquid drops with solid surfaces, National Research Council of Canada, Report No. MT-26 (May 1955).
8. C. Bonacina and S. Del Giudice, Evaporation from cryogenic liquids sprayed on flat surfaces, in *Proc. 5th Int. Heat Transfer Conf.*, Tokyo (1974).
9. I. F. Mikhaylov, G. P. Glazunov and N. A. Kosik, Evaporation of liquid-nitrogen droplets on metal surfaces, *Heat Transfer—Soviet Res.* **7**(3), 35–36 (May–June 1975).
10. John J. Daly Jr., Direct contact refrigerant freezing of foods, *ASHRAE Jl* **13**, 33–35 (June 1971).
11. J. T. Sills, Recent advances in the liquid nitrogen freezing of foods, *ASHRAE Jl* **1**, 11–17 (June 1971).
12. G. Dinglinger, Low temperature freezing of food with boiling liquids, *Kaltetechnik-Klimatisierung* **22**, 220–230 (1970).
13. L. V. Gallagher and B. S. Old, *Scient. Am.* (209), 75 (1963).
14. K. Mirua and K. Atarashiya, *et al.*, Experimental study of drying characteristics of single drops containing solids, *Heat Transfer—Japan. Res.* **1**(2), 11–17 (April–June 1972).
15. Arthur Fisher, What are we going to do about nuclear wastes?, *Popular Sci.* **213**(6), 97 (1978).
16. W. H. Nurick, J. D. Seader and T. A. Coultas, Transient heat transfer from a liquid metal spray impinging on a vertical surface, *Chem. Engng Prog. Symp. Ser., No. 59*, **61**, 127 (1965).
17. H. L. Burge, High heat flux removal by liquid metal spray cooling of surface, *Chem. Engng Prog. Symp. Ser.*, No. 59, **61**, 115 (1965).
18. C. Bonacina, G. Comini and S. Del Giudice, Evaporation of atomized liquids on hot surface, *Lett. Heat Mass Transfer* **2**, 401–406 (1975).
19. C. Bonacina, G. Comini and S. Del Giudice, Evaporazione diliquidi atomizzati a contatto di superfici calde, Quaderno No. 58, di Instituto de Fisica Tecnica, Universita di Padova (1974).
20. W.-J. Yang, Mechanics of droplet evaporation on heated surfaces, *Lett. Heat Mass Transfer* **5**, 151–155 (1978).
21. R. F. Mann and W. W. Walker, The vaporization of small binary drops on a flat plate at maximum heat flux, *Can. J. Chem. Engng* **53**, 487–493 (1975).
22. S. Toda, A study of mist cooling–thermal behaviors of liquid film formed from mist drops on a heated surface at high temperatures and high heat fluxes, *Tohoku Univ. Tech. Rep.* **36**(2), 299–350 (1971).
23. S. Toda and H. Uchida, Study of liquid film cooling with evaporation and boiling, *Heat Transfer—Japan. Res.* **2**(3), 44–62 (1973).
24. I. A. Kopchikov, G. I. Voronin, *et al.*, Liquid boiling in a thin film, *Int. J. Heat Mass Transfer* **12**, 791–796 (1969).
25. R. Messler and G. Allen, Nucleate boiling in thin films, *A.I.Ch.E. Jl* **23**, 954 (1977).
26. V. N. Murthy and P. K. Sarma, A note on thin film evaporation-prediction of heat transfer rates, *J. Chem.*

Engng Japan **6**(5), 457–459 (1973).

27. Y. Y. Hsu, F. F. Simon and J. F. Lad, Destruction of a thin liquid film flowing over a heated surface, *Chem. Engng Prog. Symp. Ser. No. 57* **61**, 139 (1965).

28. I. C. Finlay, An analysis of heat transfer during flow of an air–water mist across a heated cylinder, *Can. J. Chem. Engng* **49**, 333–339 (1971).

29. P. G. Kosky, Heat transfer to a saturated mist flowing normally to a heated cylinder, *Int. J. Heat Mass Transfer* **19**, 539 (1976).

30. I. C. Finlay, Spray flow as a heat-transfer media, *Chem. Process.* **5**, 25–29 (1971).

31. Hodgson, J. W. and J. E. Sutherland, Heat transfer from a spray-cooled isothermal cylinder, *Ind. Engng Chem. Fundls* **7**, 567–571 (1968).

32. J. G. Leidenfrost, De aquae communis nonullis qualitatibus tractatus, *Duisberg (1756)*; [English Translation: *Int. J. Heat Mass Transfer* **9**, 1153–1166 (1966)].

33. K. J. Bell, The Leidenfrost phenomenon: a survey, *Chem. Engng Prog. Symp. Ser.* **63**, 73 (1967).

34. B. S. Gottfried, C. J. Lee and K. J. Bell, The Leidenfrost Phenomenon: film boiling of liquid droplets on a flat plate, *Int. J. Heat Mass Transfer* **9**, 1167–1187 (1966).

35. Raymond E. Gaugler, Experimental investigation of spray cooling of high temperature surfaces, Ph.D. Thesis, Carnegie–Mellon University (1966).

36. Glen J. Schoessow, D. R. Jones and K. J. Baumeister, Leidenfrost film boiling of drops on a moving surface, *Chem. Engng Prog. Symp. Ser. No. 82* **64**, 95 (1968).

37. K. J. Baumeister and G. J. Schoessow, Creeping flow solution of Leidenfrost boiling with a moving surface, *Chem. Engng Prog. Symp. Ser. No. 92* **65**, 167 (1969).

38. P. S. V. K. Rao and P. K. Sarma, Effect of sub-cooling on film boiling heat transfer: droplet evaporation on a hot plate, *J. Chem. Engng Japan* **7**(5), 341–346 (1974).

39. C. J. Hoogendoorn and R. den Hord, Leidenfrost temperature and heat transfer coefficients for water spays impinging on a hot surface, *Proc. 5th Int. Heat Transfer Conf.* Tokyo (1974).

40. G. S. Emmerson, The effect of pressure and surface material on the Leidenfrost point of discrete drops of water, *Int. J. Heat Mass Transfer* **18**, 381–386 (1975).

41. G. S. Emmerson and C. W. Snoek, The effect of pressure on the Leidenfrost point of discrete drops of water and freon on a brass surface, *Int. J. Heat Mass Transfer* **21**, 1081–1086 (1978).

42. M. Cumo, G. E. Farello and G. Ferrari, Notes on droplet heat transfer, *Chem. Engng Prog. Symp. Ser. No. 92* **65**, 175 (1969).

43. L. H. J. Wachters, H. Bonne and H. J. van Nouhvis, The heat transfer from a hot horizontal plate to sessile water drops in the spherodial state, *Chem. Engng Sci.* **21**, 923–936 (1966).

44. K. J. Baumeister, G. J. Schoessow and C. E. Chmielewski, Film boiling of mercury droplets, *Can. J. Chem. Engng* **55**, 521–526 (1977).

45. W. B. Hall, The stability of Leidenfrost drops, *Proc. 5th Int. Heat Transfer Conf.* Tokyo (1974).

46. P. Savic, The cooling of a hot surface by drops boiling in contact with it, *National Research Council of Canada,* Report No. MT-37 (April 1958).

47. J. Zodrow, Results of summer research, Rice University, Mechanical Engineering Dept., private communication (August 1978).

48. W. M. Grissom, A fundamental study of spray evaporative cooling, M.S. Thesis, Rice University (1979).

49. H. S. Carslaw and J. C. Jaeger, *Conduction of Heat in Solids,* 2nd edn, p. 309. Clarendon Press, Oxford (1959).

50. V. S. Arpaci, *Conduction Heat Transfer.* Addison-Wesley, Reading, MA (1966).

APPENDIX

If the evaporation at the liquid surface caused only a one-dimensional change in the average droplet thickness, an energy balance would yield

$$K\frac{dT}{dx}\bigg|_{x=b(t)} = \rho\lambda\frac{d\hat{b}}{dt} \tag{A.1}$$

where $\hat{b}(t)$ would be the resulting one-dimensional height. However, as mass is evaporated at the surface, the edges of the droplet move inward to maintain ϕ constant. In Fig. 12(III), (A) depicts the initial droplet shape for a right circular cylinder model; (B) shows the result of a one-dimensional change; and (C) depicts the final configuration after the edges move inward.

Conservation of mass yields

$$D^2\hat{b} = \tilde{D}^2\tilde{b}. \tag{A.2}$$

Toda's analysis [22] give $b \sim d^m$. However $b = b(D)$ is what is of interest. Conservation of mass gives $4\pi d^3/3 = \pi bD^2/4$, from which $D \sim b^p$, where

$$p = \frac{1}{3}\left(\frac{3}{m} - 1\right) \tag{A.3}$$

Then, $\tilde{D} = D(\tilde{b}/b)^p$ and substitution in (A.2) gives

$$\hat{b} = \frac{\tilde{b}^{(1+2p)}}{b^{2p}}.$$

Holding b constant for the differentiation and noting that $\tilde{b} \rightarrow b$ in the limit implied by the differentiation gives

$$\frac{d\hat{b}}{dt}\bigg|_{b(t)} = (1+2p)\frac{db}{dt}. \tag{A.4}$$

Equation (A.1) then becomes

$$K\frac{dT}{dx}\bigg|_{x=b(t)} = \rho n\lambda\frac{db}{dt} \tag{A.5}$$

where $n = 1 + 2p = 3/m$.

REFROIDISSEMENT D'UNE SURFACE CHAUDE PAR UN BROUILLARD

Résumé—La plus faible température de surface possible compatible avec un refroidissement par évaporation de brouillard est déterminée expérimentalement comme une fonction linéaire du flux massique de brouillard incident. Un modèle analytique de l'évaporation de gouttelettes contrôlée par la conduction est en bon accord avec les mesures expérimentales à pression atmosphérique. Aux pressions faibles les vitesses d'évaporation décroissent significativement de telle sorte qu'il existe une pression optimum opératoire pour chaque flux surfacique de chaleur. L'initiation de "l'état Leidenfrost" fournit la limite supérieure de la température de surface pour le refroidissement par évaporation de brouillard.

FLÜSSIGKEITSSPRÜHKÜHLUNG EINER BEHEIZTEN OBERFLÄCHE

Zusammenfassung — Es wurde experimentell nachgewiesen, daß die tiefste Oberflächentemperatur, die bei der Sprühverdunstungskühlung auftreten kann, eine lineare Funktion des einwirkenden Sprühmassenstroms ist. Ein durch Wärmeleitung bestimmtes analytisches Modell der Tropfenverdunstung zeigt recht gute Übereinstimmung mit experimentellen Messungen bei Atmosphärendruck. Bei verminderten Drücken nehmen die Tropfenverdunstungsraten bedeutend ab, so daß sich für jeden gewünschten Wärmestrom an der Oberfläche ein optimaler Betriebsdruck ergibt. Der Beginn des "Leidenfrost-Zustandes" stellt die obere Grenze der Oberflächentemperatur für Sprühverdunstungskühlung dar.

АЭРОЗОЛЬНОЕ ОХЛАЖДЕНИЕ НАГРЕВАЕМОЙ ПОВЕРХНОСТИ

Аннотация — Экспериментально установлено, что самое низкое значение температуры поверхности, при котором возможно ее охлаждение, является линейной функцией массовой плотности аэрозоля. Результаты, полученные с помощью аналитической модели испарения капли, в которой передача тепла теплопроводностью играет доминирующую роль, довольно хорошо согласуются со значениями, измеренными при атмосферном давлении. При более низких давлениях скорость испарения капли значительно снижается, и для каждого заданного значения плотности теплового потока на поверхности существует определенное оптимальное рабочее давление. «Режим Лейденфроста» определяет верхний температурный предел для поверхности при испарительном аэрозольном струйном охлаждении.